

Co-feeding effect of municipal sludge on the pyrolysis of polyethylene terephthalate

Woo-Bin Lee*, Jungho Jae**, JuHye Kim*, JeongHyun Kwon*, and Young-Min Kim*^{*,†}

*Department of Environmental Engineering, Daegu University, Gyeongsan 38453, Korea

**School of Chemical and Biomolecular Engineering, Pusan National University, Busan 46241, Korea

(Received 30 May 2023 • Revised 3 August 2023 • Accepted 6 August 2023)

Abstract—The co-pyrolysis effect of municipal sludge (MS) and polyethylene terephthalate (PET) was estimated using kinetic analysis via thermogravimetric (TG) analysis and pyrolyzer-gas chromatography/mass spectrometry (Py-GC/MS). The co-feeding of MS and MS ash to PET pyrolysis decreased the PET decomposition temperature, from 427 °C to 409 °C by MS and to 420 °C by MS ash. The production amount of mono aromatic hydrocarbons (MAHs) on the pyrolysis of PET and MS was also increased by 2.5 times compared to the theoretical value by applying their co-pyrolysis. Additional use of MS ash for the co-pyrolysis of PET and MS further increased MAHs by 4.1 times compared to the theoretical value because of the radical enhancement and the catalytic effect of ash in MS. The amount of MAHs on the co-pyrolysis of PET and MS was increased by 9 times larger than the theoretical value for the co-pyrolysis of PET (0.5 mg) and MS (0.5 mg) at 500 °C by applying the increased reaction temperature (from 500 °C to 600 °C) and MS co-feeding amount (from 0.5 mg to 1.0 mg) to the pyrolysis of PET (0.5 mg).

Keywords: Municipal Sludge, Poly Ethylene Terephthalate, Pyrolysis, Ash, Aromatic Hydrocarbons

INTRODUCTION

The importance of climate change [1] and carbon neutrality [2,3] is being increasingly emphasized. To realize carbon neutrality, many countries are actively promoting waste recycling and energy conversion [4]. In the wastewater treatment process, besides decreasing energy consumption, various methods for recycling waste such as sludge have been proposed [5]. The amount of sludge generated in the waste disposal process has already increased considerably, and not only researchers but also governments of many countries have attempted to convert it into energy, rather than simply land-fill or incinerate it, by developing new technologies and policies [6,7].

Pyrolysis is a process that has been frequently attempted for producing chemical raw materials or fuels with high utility value by decomposing target wastes under medium-high temperature reduction conditions [8,9]. The effective conversion of waste polymers, such as fishing nets [10], abandoned banners [11,12], and wind turbine blades [13], over various catalysts, was also attempted in recent years.

However, in the case of sludge, compounds containing nitrogen can be generated because of the presence of proteins as the main sludge components, and the total amount of oil is less than that in plastics or biomass due to the large content of inorganics in sludges, blocking the efficient commercialization of sludge pyrolysis for fuel production [14].

Polyethylene terephthalate (PET) is one of the major polymers widely used in food containers and clothing fabrics, and the pro-

duction of PET bottles was approximately 27.64 million tons in 2018 [15]. With the help of the developed recycling technologies and policies, the PET recycling rate has risen to 31% in the USA and 52% in the European Union in 2012 and will increase further [16]; however, adequate treatment of a considerable amount of PET waste is still difficult [17]. PET is a suitable pyrolysis feedstock for the production of liquid products owing to its low mineral content and char formation after pyrolysis [18].

However, PET has an ester bond in its structure; therefore, it is highly likely to cause corrosion in the pyrolysis process by producing oil with high acidity during thermal decomposition; it also has disadvantages in that the stability of the oil itself is low [19]. Kumagai et al. [20] suggested that lowering the acid content and increasing the yield of highly stable aromatic compounds in PET thermal decomposition should be attempted, and for this purpose, decarboxylation through CaO was suggested as an alternative. Kim et al. also reported catalytic thermal decomposition of PET over waste concrete containing a large amount of CaO [21]. However, the pre- and post-thermal treatment of Ca-containing inorganics can be a cost burden on the overall PET pyrolysis process because the CaCO₃ in the catalyst must be converted to CaO to increase the decarboxylation efficiency. CaO is also converted to CaCO₃ after its use in PET pyrolysis, and it must be re-calcinated to be reused as a catalyst in PET pyrolysis [22].

The co-pyrolysis of different feedstocks, such as that involving co-feeding waste biomass and polymers like PE and PP, has been widely attempted to increase the feedstock decomposition efficiency and target product amount [23]. Although they decrease the decomposition temperature of waste plastics, noticeable changes in the product distribution in product oil are limited compared to catalytic co-pyrolysis [24].

The co-pyrolysis of sludge and PET has the potential to increase

[†]To whom correspondence should be addressed.

E-mail: ymk@daegu.ac.kr

Copyright by The Korean Institute of Chemical Engineers.

the product oil quality and stability in product oil because their co-pyrolysis can increase the feedstock decomposition efficiency, as obtained from the co-pyrolysis of sludge and other plastics [25], and the large amount of ash in sludge [26] has the potential to lead to efficient decarboxylation of acids. However, sludge and PET co-pyrolysis have not yet been attempted.

Therefore, the catalytic co-pyrolysis of municipal sludge (MS) and PET was investigated via model-free kinetic analysis using thermogravimetric (TG) analysis and pyrolyzer-gas chromatography/mass spectrometry (Py-GC/MS). The effect of the addition of MS (MS ash) to PET pyrolysis was analyzed and discussed to provide a cost-effective process for PET and MS. The synergistic effect of MS/PET co-pyrolysis on the production of mono aromatic hydrocarbons (MAHs) was evaluated by comparing the theoretical and experimental production of aromatic hydrocarbons.

EXPERIMENTAL SECTION

1. Waste Sludges and PET

Waste sludge, MS, emitted from waste treatment plants, and PET, purchased from a polymer company in South Korea, were cryo-milled with liquid nitrogen, dried in an air oven (80 °C), and sieved using a metal testing sieve (60 mesh). The physicochemical properties of the sludge and PET were analyzed by proximate and ultimate analyses.

2. TG Analysis

TG analysis was performed by applying non-isothermal heating to 6.0±0.1 mg of sludge, PET, and their mixture (sludge/PET: 1/1) from ambient temperature to 800 °C at 10 °C/min under 60 mL/min of nitrogen in a TG analyzer (TGA 55, TA Instruments).

3. Py-GC/MS Analysis

Py-GC/MS analysis was initiated by free-falling 1 mg of sludge, PET, and their mixture (sludge/PET: 1/1) into the heated pyrolyzer (Py-3030D, Frontier-Lab) at 600 °C. The pyrolysis product vapor was analyzed using GC/MS (7890A/5975, Agilent Technologies), which was directly connected to the pyrolyzer. To improve the pyrolysis product's peak sharpness, MicroJet cryo-focusing was also applied by supplying liquid nitrogen (−193 °C) to the front part of the metal capillary column (UA-5, 30 m length×0.25 mm inner diameter×0.25 μm film thickness, Frontier-Lab). Table 1 lists the other operational conditions of the Py-GC/MS. The peaks in the pyrograms were identified using NIST 8th and F-Search pyrolyzate

Table 1. Operational conditions of Py-GC/MS applied in this study

Pyrolyzer	
Pyrolyzer heater	600 °C
Interface heater	300 °C
GC/MS	
Inlet	300 °C, split 200 : 1
Oven	40 °C (2 min)→20 °C/min→280 °C (6 min)
Carrier gas	He, 1 mL/min (Constant flow mode)
MS interface	320 °C
MS scan range	m/z 29-350
Scan speed	5.4 scans/sec

libraries and integrated to compare the product amounts via peak area comparison.

RESULTS AND DISCUSSION

1. Physico-chemical Properties of MS and PET

The proximate and ultimate analysis results of MS and PET, shown in Table 2, indicated that MS has a much smaller content of volatiles due to higher ash content compared to that of PET. Although PET had a high volatile content higher than 90%, the oxygen content of PET (33.9%) was higher than that of MS (16.7%). This suggests that both sludge and PET can produce large amounts of oxygen-containing pyrolyzates as their pyrolysis product and this will necessitate the additional reforming of their pyrolysis oils [27]. The nitrogen content of MS (6.7%) also indicates that nitrogen-containing pyrolyzates can be obtained via sludge pyrolysis [28].

2. Kinetic Analysis

The TG and derivative TG (DTG) curves of MS, PET, PET/MS, PET/MS ash, and PET/MS/MS ash at 10 °C/min are shown in Fig. 1. PET had a sharp DTG peak between 370 °C and 480 °C with a maximum decomposition temperature (T_{max}) of 427 °C. After the TG analysis, approximately 10% of residual char remained, and its ash content was also much smaller than that of MS. Meanwhile, MS was decomposed in a wide temperature range, from 200 °C to 500 °C, displaying three DTG peaks. Lee et al. [14] suggested that the overlapped 1st and 2nd peaks on the MS DTG curve represent the co-pyrolysis of lipids, proteins, and carbohydrates, and the 3rd peak represents the decomposition of residual char intermediates. The low decomposition temperature of MS (1st peak) can be explained by the effective radical formation [29] and the catalytic effect of ash [30] contained largely in MS (Table 2). This suggests that the large amount of ash in MS can provide a beneficial effect by decreasing the PET decomposition temperature. As expected, the PET decomposition peak was largely shifted from 427 °C to 409 °C by co-pyrolysis with MS, confirming the synergistic effect of MS on PET decomposition during co-pyrolysis. Although the addition of MS ash (prepared by MS combustion at 600 °C) to PET also decreased the T_{max} of PET from 427 °C to 420 °C, it was higher than that for the PET and MS co-pyrolysis. This suggests that the major

Table 2. Physico-chemical properties of MS and PET

	MS [14]	PET [18]
Moisture	1.5	-
Proximate analysis (wt%) ^a	Volatiles	60.3
	Fixed carbon	7.9
	Ash	30.3
	Sum	100.0
Ultimate analysis (wt%) ^a	C	36.5
	H	7.2
	O ^b	16.7
	N	6.7
	S	1.1
	Sum	68.2
		99.9

^aOn a dry basis, ^bBy difference

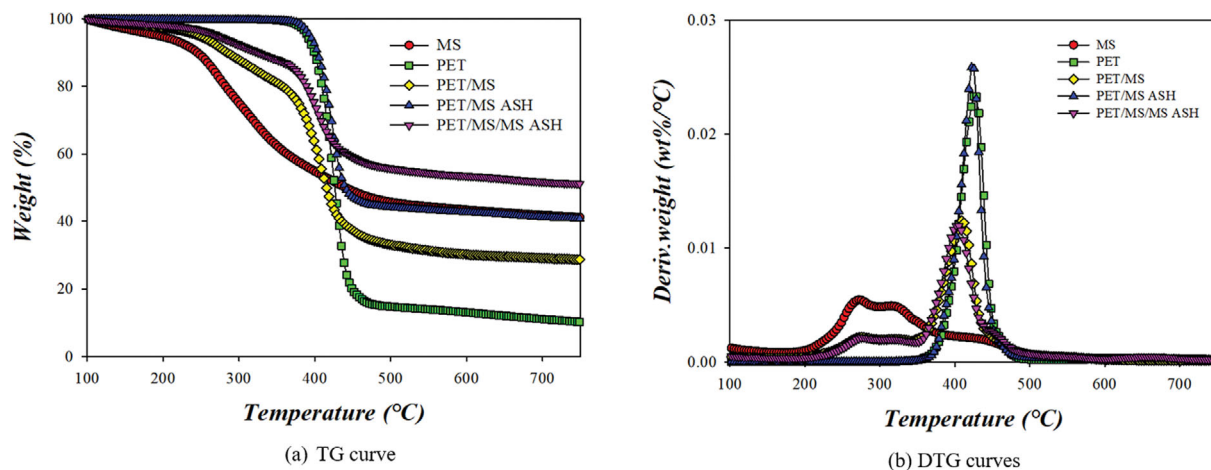


Fig. 1. TG and DTG curves obtained from the TG analysis of PET, MS, PET/MS, PET/MS ash, and PET/MS/MS ash at 10 °C/min.

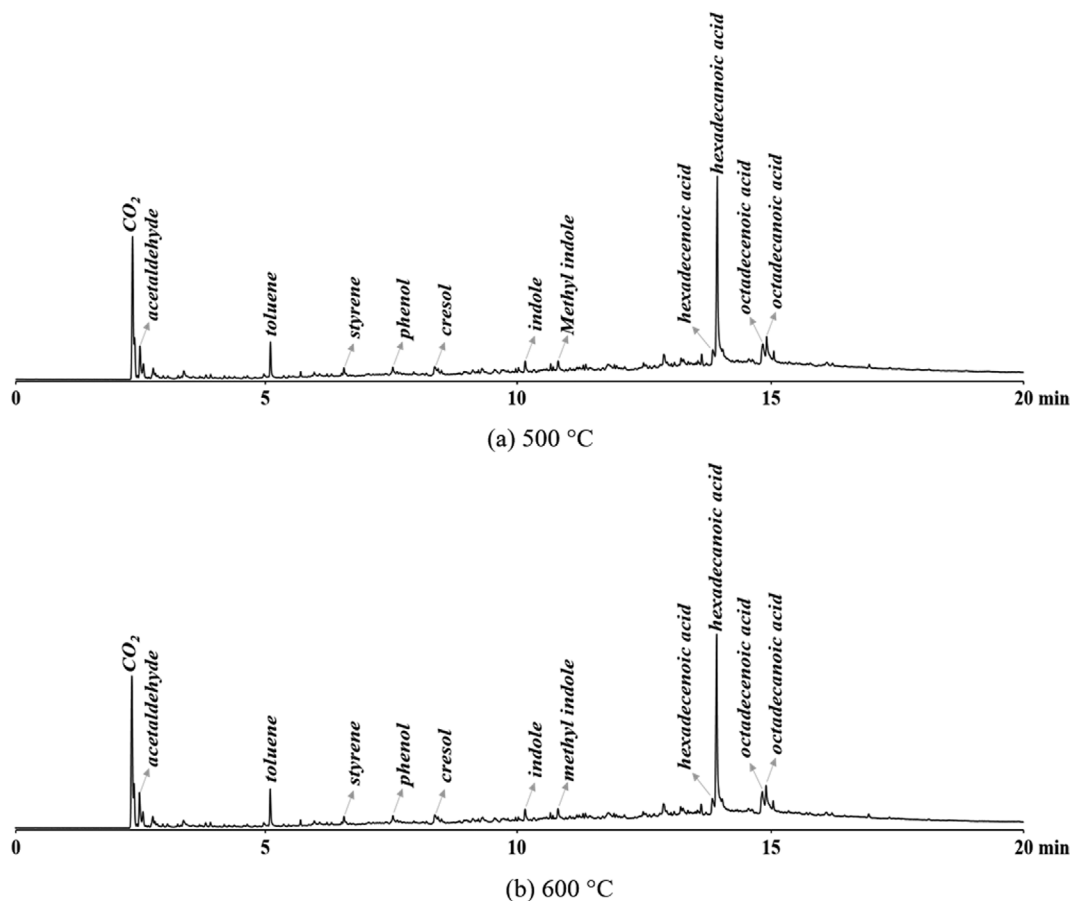


Fig. 2. Chromatograms obtained from the pyrolysis of MS at 500 °C and 600 °C.

effect on the decrease in PET decomposition temperature is caused by the effective radical formation during PET and MS co-pyrolysis. Furthermore, the addition of MS ash to the PET and MS co-pyrolysis led to an additional T_{max} decrease, reaching the lowest T_{max} (403 °C).

3. Py-GC/MS Analysis

Fig. 2 shows the pyrograms of MS (1 mg) obtained at 500 °C

and 600 °C. Both chromatograms have typical pyrolyzates of proteins [31], such as toluene, styrene, phenol, cresol, and indoles [32], and lipids [33], such as hexadecenoic acid, hexadecanoic acid, octadecenoic acid, and octadecanoic acid. Stable aromatics, such as toluene and styrene, were produced by MS pyrolysis; however, the large amounts of indoles, phenols, and fatty acids in the pyrolyzates suggest the need for additional conversion from these pyrolyza-

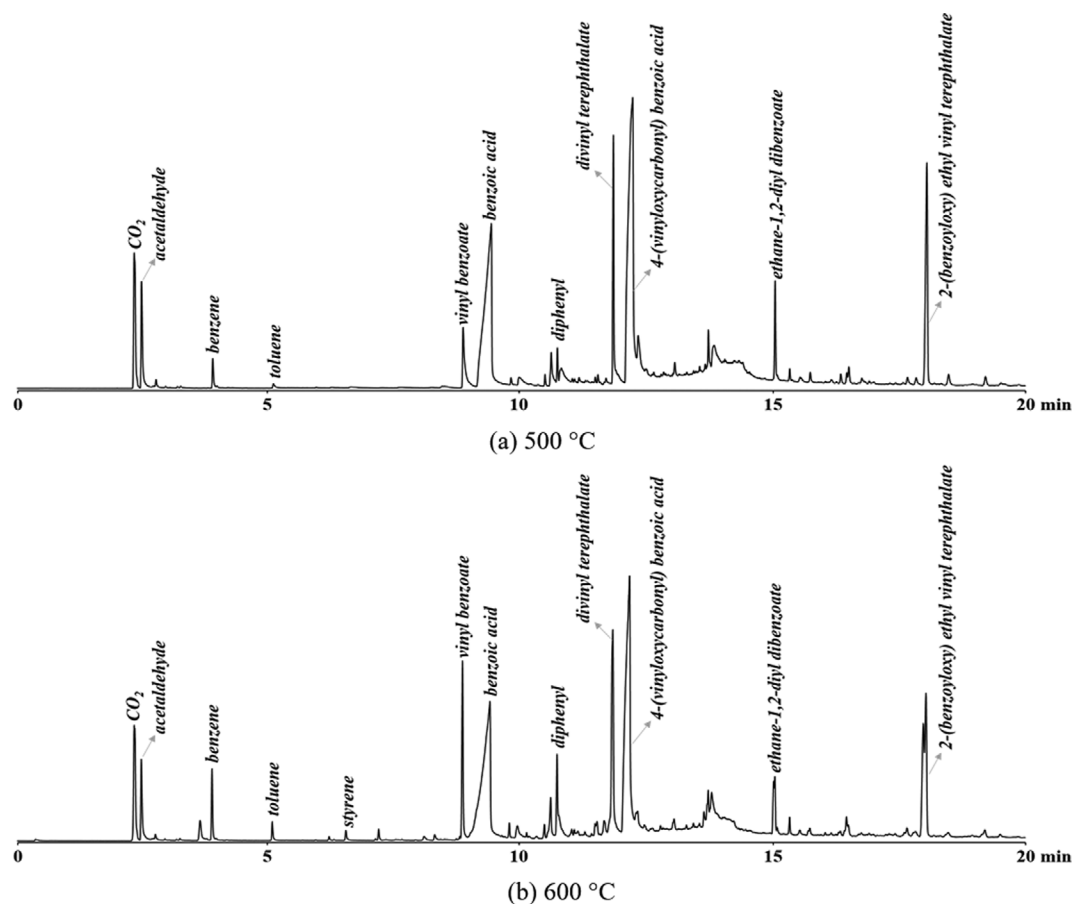


Fig. 3. Chromatograms obtained from PET pyrolysis at 500 °C and 600 °C.

Table 3. Peak intensities for the compounds obtained from the Py-GC/MS analysis of PET, MS, PET/MS, and PET/MS/MS ash (Unit: Peak area $\times 10^{-6}$)

Compound	PET (1 mg)	MS (1 mg)	PET+MS ¹ (1 mg)		PET+MS+MS ash ² (1.5 mg)
			Theo.	Exp.	
Carbon dioxide	191	123	157	180	197
Acetaldehyde	137	29	83	96	113
Benzene	27	N.D.	13	68	128
Toluene	9	28	19	24	26
Styrene	7	8	8	8	10
Vinyl benzoate	118	N.D.	59	28	24
Benzoic acid	853	0	426	424	402
Indole	N.D.	11	6	N.D.	N.D.
Diphenyl	127	N.D.	63	36	59
Methyl indole	N.D.	15	7	N.D.	N.D.
Divinyl terephthalate	243	N.D.	121	36	17
4-(Vinylloxycarbonyl) benzoic acid	987	N.D.	494	181	15
Fatty acids ³	N.D.	285	143	163	38
Ethane-1,2-diyl dibenzoate	109	N.D.	55	23	40
2-(Benzoyloxy) ethyl vinyl terephthalate	294	N.D.	147	55	39

¹PET/MS: 1/1.

²PET/MS/MS ash: 1/1/1.

³Hexadecenoic acid, Hexadecanoic acid, Octadecenoic acid, and Octadecanoic acid.

N.D.: Not detected.

tes to stable aromatics to prevent NO_x formation [34] and increase oil stability [35]. Although higher temperature pyrolysis led to a decrease in fatty acids, no noticeable change in the product distribution obtained from MS pyrolysis at 600 °C was observed compared to that at 500 °C.

The pyrograms of PET (1 mg) obtained at 500 °C and 600 °C are shown in Fig. 3. As expected, PET produces large amounts of benzoate and benzoic acid [36]. In addition, PET pyrolysis oil consists of large molecular pyrolyzates such as divinyl terephthalate, 4-(vinylloxycarbonyl) benzoic acid, ethane-1,2-diyl dibenzoate, and 2-(benzoyloxy)ethyl vinyl terephthalate, resulting in high viscosity and acidity [19]. Although these large molecular pyrolyzates were decreased by increasing the reaction temperature from 500 °C to 600 °C, no large increase in stable MAHs, such as benzene and toluene, was obtained, suggesting the need for additional cracking using catalysts.

Fig. 4 shows the pyrograms obtained from the co-pyrolysis of PET, MS, and MS ash at 500 °C. Although PET and MS co-pyrolysis produced the same types of pyrolysis products of MS and PET pyrolysis, their distribution was largely different. The relative intensities of large molecular pyrolyzates of PET, such as divinyl terephthalate, 4-(vinylloxycarbonyl) benzoic acid, ethane-1,2-diyl dibenzoate, and 2-(benzoyloxy) ethyl vinyl terephthalate, obtained from the co-pyrolysis of PET (0.5 mg) and MS (0.5 mg) were much smaller than the half of the peak intensities of those obtained from the pyroly-

sis of PET (1 mg). Additionally, the peak intensities for small molecular carbon dioxide, acetaldehyde, and MAHs (benzene, toluene, styrene) were much larger than their theoretical values (Table 3), suggesting their synergistic formation due to their co-pyrolysis. Interestingly, the addition of MS ash to the catalytic PET and MS co-pyrolysis largely increased the amount of benzene and diphenyl produced, confirming the catalytic effect of MS ash on the production of aromatic hydrocarbons. High content of Ca, P, Mg, and K in MS ash [37] can facilitate effective deoxygenation, increasing the formation of aromatic hydrocarbons via the decarboxylation of benzoic acid, divinyl terephthalate, 4-(vinylloxycarbonyl) benzoic acid, ethane-1,2-diyl dibenzoate, and 2-(benzoyloxy) ethyl vinyl terephthalate [22].

The formation efficiency of MAHs was also further increased by elevating the reaction temperature from 500 °C to 600 °C because of the increased cracking efficiency, which was maximized by increasing the co-feeding amount of MS to PET pyrolysis at 600 °C, as shown in Fig. 5. Reaction temperature is an important factor influencing the pyrolysis quality because high temperature can lead to more effective cracking of oxygen-containing and nitrogen-containing compounds, leading the effective radical condensation on the co-pyrolysis [38]. The further increase of MAHs by increasing MS co-feeding amount at 600 °C can confirm that the increased radical formation from MS at the elevated temperature and a larger amount of inorganics in MS can lead to the additional conversion

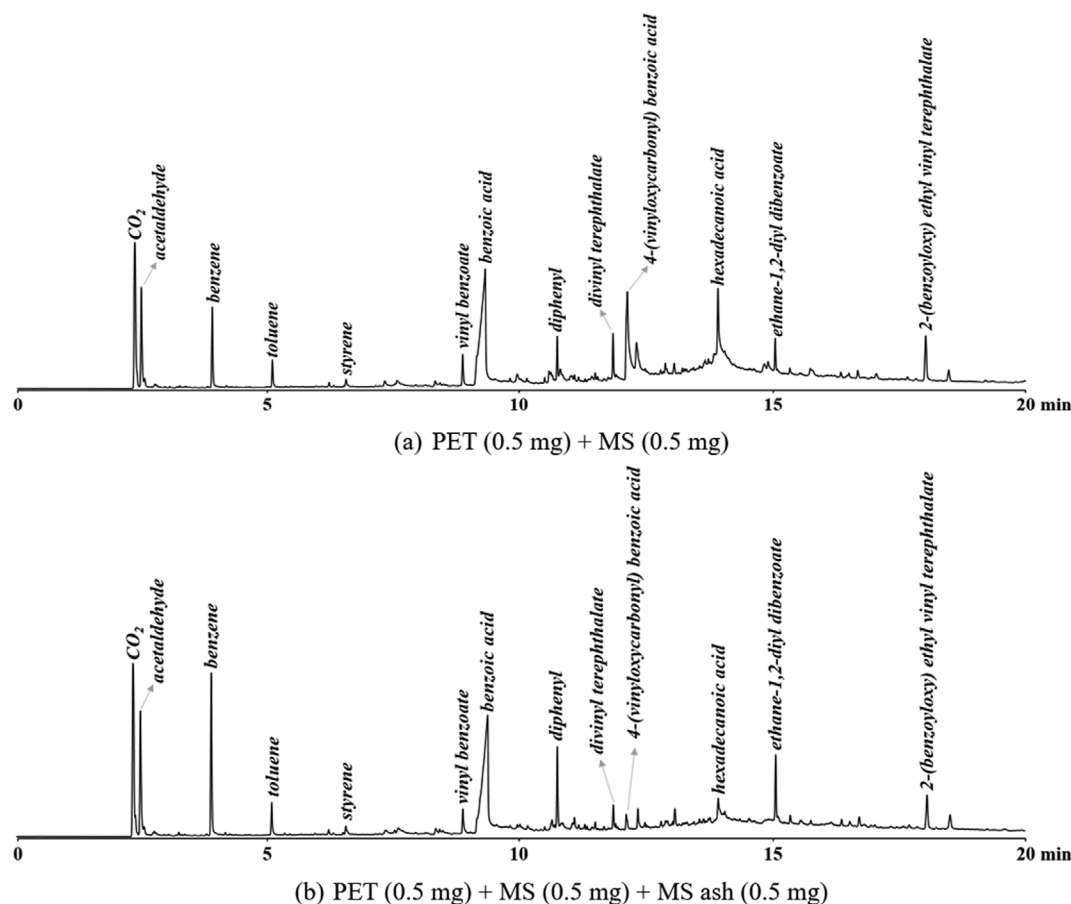


Fig. 4. The co-feeding effect of MS and MS ash on the pyrolysis of PET at 500 °C.

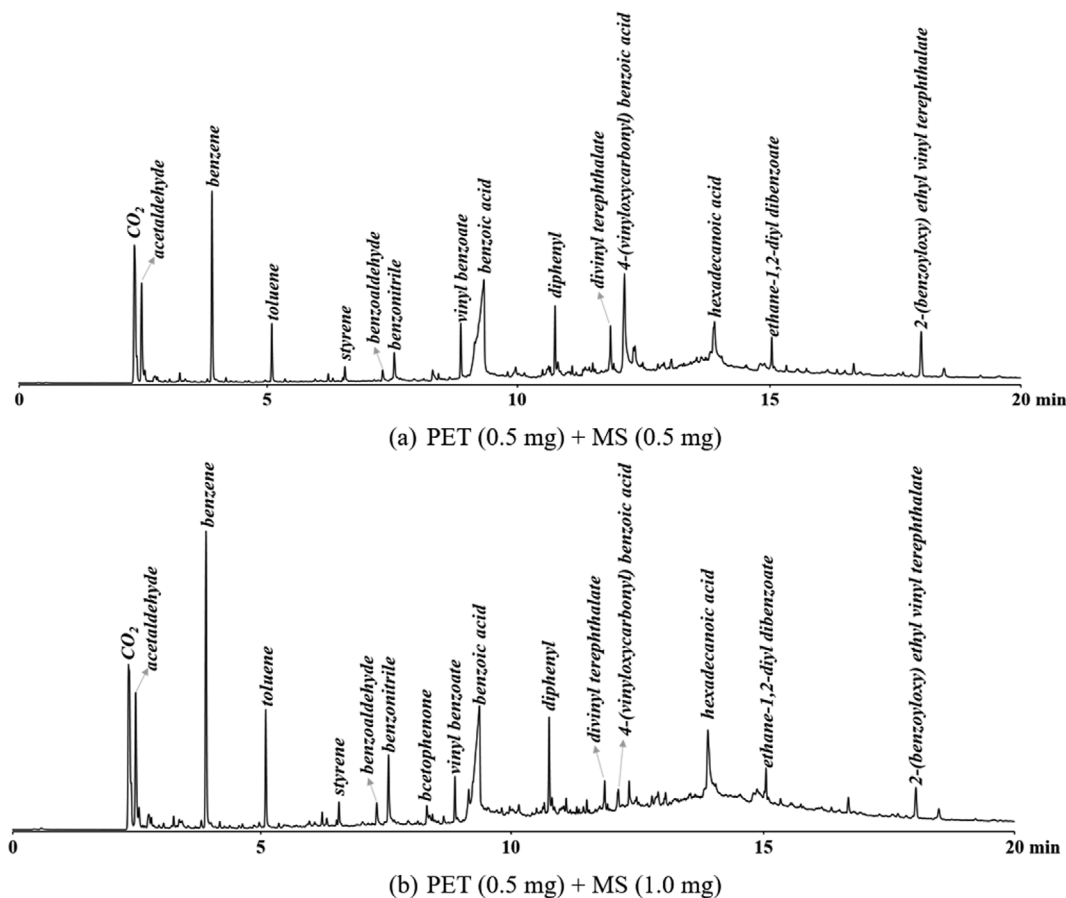


Fig. 5. The co-feeding effect of MS on the pyrolysis of PET at 600 °C.

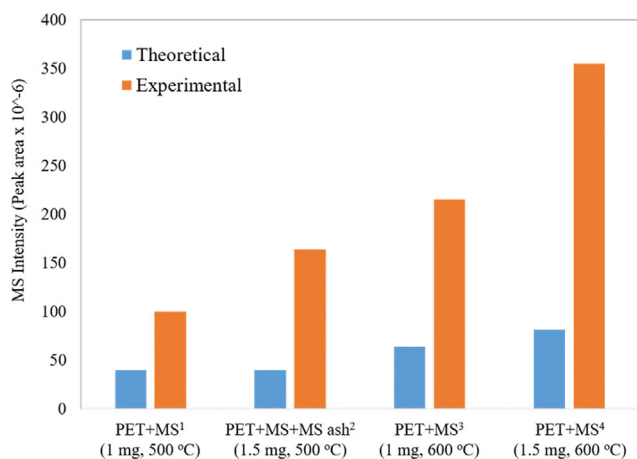


Fig. 6. Theoretical and experimental amount of MAHs for the co-pyrolysis of PET, MS, and MS ash at different reaction temperatures (¹PET/MS: 1/1, ²PET/MS/MS ash: 1/1/1, ³PET/MS: 1/1, ⁴PET/MS: 1/2).

of large molecular PET pyrolyzates to MAHs more effectively.

The theoretical and experimental MS intensities for MAHs are compared in Fig. 6. As expected, experimental MAHs amounts in all experiments were much larger than the theoretical values from 2.5 by the co-pyrolysis of PET (0.5 mg) and MS (0.5 mg) at 500 °C

to 4.4 times by that of PET (0.5 mg) and MS (1.0 mg) at 600 °C, confirming the synergistic MAHs formation on the co-pyrolysis of PET and MS. Compared to the co-pyrolysis of PET (0.5 mg) and MS (0.5 mg) at 500 °C, MAHs production amount was increased up to 9 times larger by increasing temperature to 600 °C and MS co-feeding amount to 1.0 mg, suggesting the feasibility of co-feeding of MS to PET pyrolysis.

CONCLUSIONS

The co-treatment effect of MS and PET, not only for proper treatment but also for producing value-added fuels, mono aromatic hydrocarbons, was proven in this study. Although no noticeable change was observed in the decomposition temperature and product distribution of MS, a large decrease in T_{max} for PET decomposition was achieved with the synergistic production of aromatic hydrocarbons by applying simple MS and PET co-pyrolysis. Effective radical enrichment and the catalytic effect of inorganics in MS on MS and PET co-pyrolysis led to more effective PET decomposition and increased aromatic production. MAHs amount, produced on the co-pyrolysis of PET (0.5 mg) and MS (0.5 mg) at 500 °C, was increased up to maximum 9 times larger value by increasing reaction temperature from 500 to 600 °C and MS co-feeding amount from 0.5 mg to 1.0 mg, confirming the importance of reaction parameter optimization on the co-pyrolysis of PET and MS.

ACKNOWLEDGEMENTS

This study was supported by a National Research Foundation of Korea (NRF) grant funded by the Korean government (MSIT) (NRF-2020R1A5A1019631).

REFERENCES

1. D. Lee, H. Nam, M. W. Seo, S. H. Lee, D. Tokmurzin, S. Wang and Y.-K. Park, *Chem. Eng. J.*, **447**, 137501 (2022).
2. P. Bhavani, D. P. Kumar, M. Hussain, T. M. Aminabhavi and Y.-K. Park, *Chem. Eng. J.*, **434**, 134743 (2022).
3. S. Jung, Y.-K. Park and E. E. Kwon, *J. CO₂ Util.*, **32**, 128 (2019).
4. J.-Y. Kim, S. Oh and Y.-K. Park, *J. Hazard. Mater.*, **384**, 121356 (2020).
5. A. Ding, R. Zhang, H. H. Ngo, X. He, J. Ma, J. Nan and G. Li, *Sci. Total Environ.*, **769**, 144451 (2021).
6. M. Y. Seo, D. Tokmurzin, D. Lee, S. H. Lee, M. W. Seo and Y.-K. Park, *Bioresour. Technol.*, **361**, 1227740 (2022).
7. P. Bhavani, M. Hussain and Y.-K. Park, *J. Clean. Prod.*, **330**, 129899 (2022).
8. Y.-K. Park, J. S. Jung, J. Jae, S. B. Hong, A. Watanabe and Y.-M. Kim, *Chem. Eng. J.*, **377**, 119742 (2019).
9. M. W. Seo, S. H. Lee, H. Nam, D. Lee, D. Tokmurzin, S. Wang and Y.-K. Park, *Bioresour. Technol.*, **343**, 126109 (2022).
10. S. Kim, Y. T. Kim, L. S. Oh, H. J. Kim and J. Lee, *J. Mater. Chem. A*, **10**, 20024 (2022).
11. C. Park, H. Lee, N. Lee, B. Ahn and J. Lee, *J. Hazard. Mater.*, **440**, 129825 (2022).
12. W. Yang, K.-H. Kim and J. Lee, *J. Clean. Prod.*, **276**, 134292 (2022).
13. N. Lee, K. A. Lin and J. Lee, *Environ. Res.*, **213**, 113560 (2022).
14. S. Lee, Y.-M. Kim, M. Z. Siddiqui and Y.-K. Park, *Environ. Pollut.*, **285**, 117197 (2021).
15. N. A. Al-Thani, T. Al-Ansari and M. Haouari, *Heliyon*, **8**, e10274 (2022).
16. A. Singh, S. L. Banerjee, K. Kumari and P. P. Kundu, *Handbook of Solid Waste Manag.*, Springer, Singapore, 1149 (2022).
17. N. Evode, S. A. Qamar, M. Bilal, D. Barceló and H. M. N. Iqbal, *Case Stud. Chem. Environ. Eng.*, **4**, 100142 (2021).
18. Y.-K. Park, J. Jung, S. Ryu, H. W. Lee, M. Z. Siddiqui, J. Jae, A. Watanabe and Y.-M. Kim, *Appl. Energy*, **250**, 1706 (2019).
19. M. Fukushima, B. Wu, H. Ibe, K. Wakai, E. Sugiyama, H. Abe, K. Kitagawa, S. Tsuruga, K. Shimura and E. Ono, *J. Mater. Cycles Waste Manag.*, **12**, 108 (2010).
20. S. Kumagai, R. Yamasaki, T. Kameda, Y. Saito, A. Watanabe, C. Watanabe, N. Teramae and T. Yoshioka, *Chem. Eng. J.*, **332**, 169 (2018).
21. S. Lim and Y.-M. Kim, *Appl. Chem. Eng.*, **30**, 707 (2019).
22. S. Kumagai, R. Yamasaki, T. Kameda, Y. Saito, A. Watanabe, C. Watanabe, N. Teramae and T. Yoshioka, *Energy Fuels*, **34**, 2492 (2020).
23. B.-S. Kim, Y.-M. Kim, H. W. Lee, J. Jae, D. H. Kim, S.-C. Jung, C. Watanabe and Y.-K. Park, *ACS Sustainable Chem. Eng.*, **4**, 1354 (2016).
24. Y.-M. Kim, J. Jeong, S. Ryu, H. W. Lee, J. S. Jung, M. Z. Siddiqui, S.-C. Jung, J.-K. Jeon, J. Jae and Y.-K. Park, *Energy Convers. Manag.*, **195**, 727 (2019).
25. Z. Ai, W. Zhang, L. Yang, H. Chen, Z. Xu, L. Leng and H. Li, *J. Anal. Appl. Pyrolysis*, **166**, 105610 (2022).
26. B. Wang, Y. Liu, Y. Guan and Y. Feng, *J. Clean. Prod.*, **334**, 130224 (2022).
27. H. Jia, H. Ben, Y. Luo and R. Wang, *Polymers*, **12**, 705 (2020).
28. X.-Y. Zhao, W. Jiang, Y.-F. Shan and J.-P. Cao, *Energy Fuels*, **36**, 502 (2022).
29. W. W. Nawar, *J. Chem. Educ.*, **61**, 299 (1984).
30. E. Quiroga, J. Molto, J. A. Conesa, M. F. Valero and M. Cobo, *Catalysts*, **10**, 508 (2020).
31. Y.-M. Kim, T. U. Han, B. Lee, A. Watanabe, N. Teramae, J.-H. Kim, Y.-K. Park, H. Park and S. Kim, *Algal Res.*, **32**, 60 (2018).
32. S. Tsuge and H. Matsubara, *J. Anal. Appl. Pyrolysis*, **8**, 49 (1985).
33. D. I. Sánchez-Machado, J. López-Cervantes, J. López-Hernández and P. Paseiro-Losada, *Food Chem.*, **85**, 439 (2004).
34. H. Chen, R. Shan, F. Zhao, J. Gu, Y. Zhang, H. Yuan and Y. Chen, *Chem. Eng. J.*, **451**, 138979 (2023).
35. L. Leng, L. Yang, J. Chen, S. Leng, H. Li, H. Li, X. Yuan, W. Zhou and H. Huang, *Bioresour. Technol.*, **315**, 123801 (2020).
36. N. Dimitrov, L. K. Krehula, A. P. Siročić and Z. Hrnjak-Murgić, *Polym. Degrad. Stab.*, **98**, 972 (2013).
37. S. Werle and M. Dudziak, *Energies*, **7**, 462 (2014).
38. B. A. Mohamed, L. Y. Li, *Environ. Chem. Lett.*, **21**, 153 (2023).